REGION-OF-INTEREST TOMOGRAPHY USING MULTIRESOLUTION INTERPOLATION

Daniel Pak-Kong Lun and TaiChiu Hsung
Department of Electronic Engineering,
The Hong Kong Polytechnic University,
Hung Hom, Hong Kong.

ABSTRACT

The wavelet localization technique was recently applied to the application of Region-of-Interest tomography. It achieves a significant saving in the required projections if only a small region of a tomographic image is of interest. In this paper, we firstly show that, with the same sampling requirement, a simple interpolation scheme applied on the samples can give a result at least as good as that achieved by using the wavelet localization approach. It means that we can use a much simple approach to achieve the same performance. Second, we propose a new sampling scheme such that the required projections of each angle are further reduced in a multiresolution form. With this sampling scheme, more than 84% of projections are saved to reconstruct a 32x32 pixels region of a 256x256 pixels image. The signal-to-error ratio of the reconstructed region-of-interest is over 50dB as compare with the case of full projection. Moreover, we also investigate the effect of applying the interlaced sampling scheme on the proposed method. It is seen that a further reduction in the sampling requirement can be achieved although a slight decrease in signal-to-error ratio may result.

1. INTRODUCTION

Region-of-Interest (ROI) tomography, which refers to the techniques used in reconstructing tomographic images localized to an interested region, has aroused much interest recently [1, 2, 3, 4]. It suggests that if only a small region of a tomographic image is of interest, essentially only the projections localized to this ROI are required for its reconstruction. It has important consequences to both the transmission and emission tomography. For transmission tomography, it implies that less x-ray dose is required to reconstruct the ROI. For emission tomography, it implies that a higher resolution ROI can be obtained by placing more detecting cameras within the support of the ROI.

The study on the Region-of-Interest tomography has been conducted in different directions[1, 2, 3, 4]. Nevertheless, it has been shown that the ROI cannot be exactly reconstructed with only the projections localized to the ROI [3, 4]. Recent study in this area is then mainly on how to minimize the projections other than the localized ones. The exponential sampling approach [4] tries to minimize the projection in radial direction, whereas the wavelet localization approach [1, 2] concentrates on reducing the projections angularly.

In this paper, we first make an analysis on the wavelet localization approach and show that a simple linear interpolation on the projections can give a result as good as that achieved by the wavelet localization approach. Further to this work, we propose a new sampling scheme such that the required projections of each angle are reduced in a multiresolution form. It is possible due to the observations that, when the projections of a particular angle are down sampled into a multiresolution form, the aliasing problem will not occur or will be negligible for the samples of some of the resolutions. The reduced projections are then interpolated in a multiresolution way. Standard reconstruction technique is applied on the interpolated projections to obtain a tomographic image. As a result, a more than 84% saving in the required projections is achieved. The reconstructed ROI has an over 50dB signal-to-error ratio as compared with that using full projection data set.

2. WAVELET LOCALIZATION OF THE RADON TRANSFORM

The process of tomographic imaging can be mathematically modeled by using the Radon transform [5]. The definition of the Radon transform of a function $f : R^2 \rightarrow R$ is shown as follows:

$$P_f(\vec{\theta}, t) = \int_R f(\vec{x})\delta(t - \vec{\theta} \cdot \vec{x})d\vec{x} \qquad (1)$$

Eqn.1 states that $P_f(\vec{\theta}, t)$ is the line integral of f through $\vec{x} \in R^2$ and perpendicular to $\vec{\theta}$. The function f can be recovered from the projection using the inverse Radon transform defined as in eqn.2.

$$f(\vec{x}) = \int_S F P_f(\vec{\theta}, \vec{\theta} \cdot \vec{x})d\vec{\theta} \qquad (2)$$

where the function F represents the ramp filter used in the reconstruction and the outer integration can be considered as the backprojection. This is the well-known filtered backprojection algorithm used in tomographic image reconstruction. Due to the discontinuity of the transfer function of the ramp filter at d.c., the impulse response of the ramp filter is never compact. This implies that even if one tries to reconstruct a small part of the function f, the non-compact characteristic of the ramp filter requires that all projections P_f from every angle should be available for the reconstruction. However, the effect due to the discontinuity of the ramp filter can be minimized if the function f has zero d.c. response and several vanishing moments[5]. It is known that many wavelet functions have these properties. Assume that we perform the wavelet transform on the projections of each angle such that the wavelet coefficients $d_{j,n}$ are obtained on scale j and translation n at angle θ and the scaling coefficient $c_{J,n}$ are obtained on scale J and translation n at angle θ, eqn.2 can be rewritten as follows:

$$\begin{aligned} f(\vec{x}) = \; & \int_S \sum_{j=0}^{J} \sum_n d_{j,n}(\vec{\theta}) F\left(\psi_{j,n}(\vec{\theta} \cdot \vec{x})\right) \\ & + \sum_n c_{J,n}(\vec{\theta}) F\left(\phi_{J,n}(\vec{\theta} \cdot \vec{x})\right) d\vec{\theta} \end{aligned} \qquad (3)$$

where ψ and ϕ are the wavelet function and scaling function, respectively. The equality of eqn.3 holds because of the

linearity of the ramp filter F. For those wavelet function ψ that has several zero moments, the locality properties of the wavelets will be preserved after it is convolved with the ramp filter F. Hence for those wavelets, we need only local information to perform the inversion. However, only the high resolution wavelet function ψ have enough zero moments, the others will have increasingly large support, and so will their filtered versions. Hence for those wavelets, we still need to project the whole object even a small region is of interest. Fortunately, it was shown that [1, 2] for those wavelets, the wavelet coefficients $d_{j,n}$ are essentially band-limited. It enables one to compute them from the nonlocal data for only a few angles and interpolate the values of these coefficients at the other necessary angles. In this way, the overall sampling requirement is reduced. The procedure of reconstruction using the wavelet approach [1] is summarized in an example shown in fig.1a and the required sampling pattern is shown in fig.1b.

3. REPLACING THE WAVELET TRANSFORM BY INTERPOLATION

We show in this section that only if the same sampling pattern as the wavelet approach is used, we can reconstruct the region-of-interest with a quality at least as good as that of the wavelet approach by simply interpolating the reduced projections. This implies that less computation effort is required since we need not perform the wavelet transform. Without loss of generality, we use the example in fig.1a to illustrate the idea.

First, let us consider the input requirement of the wavelet and scaling filters in fig.1a. It is seen that the wavelet filter requires only the local projections of every angle, while the scaling filter requires full projections of only every other angles. As the wavelet function is compact support, it is obvious that there will not be any negative effect to the reconstructed image if we combine the sampling requirements of both the wavelet and scaling filters such that the inputs to them are the same.

Second, let us further consider the scaling coefficients generated by the scaling filter. It was suggested in [1] that interpolation should be performed on these scaling coefficients to estimate those unknown coefficients of the missing angles. However, it can be easily shown that, due to the linearity of the wavelet transform, any linear interpolation performed on the scaling coefficients of a particular scale is not necessary if the same interpolation has been done in the projection domain, that is, before the wavelet transform. For instance, consider the following linear interpolator applied on the scaling or the wavelet coefficients of any resolution:

$$d_{j,n}(\theta_i) = \sum_{k\in S_1}\sum_{n'\in Z} A_j(k,n') d_{j,n+n'}(\theta_k) \quad i \in S_2$$
$$c_{J,n}(\theta_i) = \sum_{k\in S_1}\sum_{n'\in Z} A_J(k,n') c_{J,n+n'}(\theta_k) \quad i \in S_2 \qquad (4)$$

For a particular resolution j, $S_1 \subset Z$ such that the wavelet or scaling coefficients of $\theta_i : i \in S_1$ is known, while $S_2 \subset Z$ such that the wavelet coefficients of $\theta_i : i \in S_2$ is unknown. The parameter $A \in R$ describes the interpolator. Assume that the wavelet and scaling coefficients are obtained by applying the discrete wavelet transform on the projections as follows:

$$\begin{aligned} d_{j,n}(\vec{\theta}) &= \left\langle P_f(\vec{\theta},t), \tilde{\psi}_{j,n}(t)\right\rangle \\ &= a_o^{j/2}\int P_f(\vec{\theta},t)\tilde{\psi}(a_o^j r - nb_o)dt \\ c_{J,n}(\vec{\theta}) &= \left\langle P_f(\vec{\theta},t), \tilde{\phi}_{J,n}(t)\right\rangle \\ &= \int P_f(\vec{\theta},t)\tilde{\phi}(a_o^J t - nb_o)dt \qquad (5) \end{aligned}$$

where $r \in R; a_o, b_o \in R$ are two constants which define the sampling lattice of the wavelet transform. Substitute eqn.5 into eqn.4 and rearrange the summations and integrations, we have

$$d_{j,n}(\theta_i) \simeq < [\sum_{k\in S_1}\sum_{n'\in Z} A_j(k,n') P_f(\theta_k, t+n'b_o a_o^{-j})], \psi_{j,n}(t) >$$
$$c_{J,n}(\theta_i) \simeq < [\sum_{k\in S_1}\sum_{n'\in Z} A_J(k,n') P_f(\theta_k, t+n'b_o a_o^{-J})], \phi_{J,n}(t) > \qquad (6)$$

Eqn.6 shows that the interpolation of the scaling or wavelet coefficients can be replaced by performing the same interpolation on some selected projections and then applying the wavelet transform on the interpolated projections. Based on the above arguments, fig.1a can be modified as in fig.2 where the blocks WT and IWT can be canceled out. Hence the final proposal is just simply as follows:

1. Obtain the projection with a pattern as in fig.1b;
2. interpolate the missing projection; and
3. perform filtered backprojection.

The above approach can be extended to the case when a multi-level wavelet transform is used. Although the above approach is very simple, the result is surprisingly good. Figs.3c and 3d show a comparison of using the modified approach and the original wavelet localization approach to reconstruct a region-of-interest of 32x32 pixels at the centre of a 256x256 pixels image. Figs.3a and 3b show the reduced sinogram used in both approaches and reconstructed image from full samples respectively. For the modified approach, a simple linear interpolation is performed on the reduced sinogram to estimate the missing projections. Both approaches achieve a signal-to-error ratio of over 50 dB in reconstructing the region-of-interest. However the modified approach does not require to perform the wavelet transform. Furthermore for the region other than the interested one, the quality of reconstruction using the modified approach is better than the wavelet localization approach. This result shows that the sampling pattern is the most crucial factor to reconstruct the region-of-interest. Once a suitable sampling pattern is used, the subsequent operation can be so simple that even a linear interpolation would allow a satisfactory reconstructed image.

4. NEW SAMPLING SCHEME

Indeed, the sampling requirement in figure 1.b can be further reduced by decimating the radial samples of each angle in a multiresolution form. It is well known that due to the bowtie support of the Fourier transform of a sinogram, a reduction of the radial sampling rate may cause the problem of aliasing. However, it is observed that the Fourier support of a sinogram is essentially supported up to 1/2 of the spectrum, while the power of the spectrum is concentrated at the central 1/8 region of the bowtie. Therefore, the aliasing components that are introduced to the central 1/8 of the bowtie due to a decimation of the radial samples will not be significant, unless the decimation rate is higher than 8. Recall a multi-level implementation of the wavelet localization approach, the most detailed part of the reconstructed image is generated by the highest resolution wavelets. Since the highest details inside the ROI is of interest, no decimation is allowed in the radial samples of the highest resolution wavelet components. However, due to the locality of the ramped wavelet, we only require local projection samples for the ROI plus the support of the ramped wavelet filter.

For the next highest resolution wavelet function, since only the part that belongs to the lower 1/2 frequency spectrum of the image is generated, we can decimate the radial samples by two without introducing aliasing problem. However, the spatial support of the next highest resolution wavelet function is doubled and therefore local projection samples of ROI plus twice the support of the ramped wavelet filter are required.

For the next resolution wavelet function, it is surprising to observe that the output from this wavelet has very little effect to the quality of the final image. It may due to the following two reasons: 1) The images reconstructed from the highest two resolution wavelet functions have covered 75% of the Fourier spectrum of the final image. In terms of the magnitude of the spectral power, the output of this wavelet function is also negligible as compared with that given by the scaling function. 2) As the resolution of the wavelet function is decreasing, the lower frequency part of the image will be generated. During the ramp filtering, the low frequency part will be suppressed and hence the output from this wavelet function contributes very little to the quality of image inside the ROI. Consequently, the output of this resolution can be excluded from the final reconstruction without significantly affecting the reconstructed image quality.

Finally for the scaling function, since the lowest 1/8 spectrum of the image is generated by the scaling function, its output cannot be ignored. As it is discussed before, since the magnitude of the signal power in this part is so high, aliasing components due to the decimation of radial samples has negligible effect to its magnitude, unless the decimation rate is greater than 8. Hence an input with radial samples which is decimated by 8 can be applied to the scaling function without introducing the aliasing problem. Due to the bandlimited feature of the scaling function as discussed in section 2, we can also decimate the angular samples by 8 as well. However, since the scaling function is globally supported, projections need to be performed for the whole object irrespective to the size and location of the ROI.

Combining all the sampling requirements as stated above, a new sampling scheme is shown in figure 5a. The radial samples are taken in a multiresolution form and the angular samples are taken as in the wavelet localization approach. For this sampled sinogram, we may use the wavelet localization approach to reconstruct the ROI. However, as it is described above that a projection domain interpolation can perform at least as good as the wavelet localization approach, hence we propose the following multiresolution interpolation algorithm in the projection domain,

1. Obtain projection sample as in figure 5a.
2. Re-sample the sinogram to an MxM sinogram.
3. Interpolate up to 2Mx2M using the framework of 2D multi-resolution analysis.
4. Superimpose the interpolated sinogram with 2M projection samples which are localized in ROI plus length of ramped wavelet filter.
5. Repeat steps 3 and 4 with doubled M until an NxN image is obtained.

The outline of the algorithm is shown in figure 4. The interpolating filter we used is the Deslauriers-Dubuc filter of order 4 [6], $[-2^{-5}, 0, 9\cdot 2^{-5}, 2^{-1}, 9\cdot 2^{-5}, 0, -2^{-5}]$. This class of interpolating filters are symmetric with most compact support, they have the properties:

$$h(w) + h(w+\pi) = 1, \;\; h(w) = h(-w) \qquad (7)$$

We applied the above algorithm on a sinogram with 256 angles and 256 samples per angle. The sampled sinogram and the results obtained using the multiresolution interpolation can be seen from figure 5b,5c respectively. The signal-to-error ratio of the ROI using the multiresolution interpolation is 64.35dB as compared with the full sample reconstruction.

Furthermore, we can also apply the interlaced sampling scheme on our proposed multiresolution interpolation method to further increase the sampling saving. The sampling pattern of the new interlaced ROI sampling scheme and the sampled sinogram are shown in figure 5d and 5e respectively. We interpolate the interlaced sinogram using the proposed multiresolution interpolation algorithm as shown above. The interpolated sinogram is then used to reconstruct the image using the standard filtered backprojection algorithm. The result is shown in figure 5f. As it is expected that the signal-to-error ratio drops slightly as the samples required are much less than the previous proposed approach. Nevertheless, the error in the ROI can hardly be visually identified.

5. CONCLUSION

In this paper, we have shown that, with the same sampling requirement, a simple interpolation scheme applied on the reduced projections can give a result at least as good as that achieved by the wavelet approach for the localization of the Radon transform. This implies that the wavelet transform may not be necessary in the reconstruction process, hence the computational complexity can be reduced. Second, we propose a new sampling scheme such that the required projections are further reduced by decimating the required projections of each angle in a multiresolution form. With this sampling scheme, more than 84% of projections are saved to reconstruct a 256x256 pixels image with the region-of-interest located at the centre 32x32 pixels. The signal-to-error ratio of the reconstructed region-of-interest is over 50dB as compared with the case of full projection. Moreover, we also investigate the effect of applying the interlaced sampling approach on the proposed method. It is seen that a further saving in the sampling requirement can be achieved although a slight decrease in signal-to-error ratio may result.

REFERENCES

[1] Joe DeStefano and Tim Olson. "Wavelet Localization of the Radon Transform". *IEEE Transactions on Signal Processing*, 42(8):2055–2067, 1994.

[2] Alexander H. Delaney and Yoram Bresler. "Multiresolution Tomographic Reconstruction Using Wavelets". *IEEE Transactions on Image Processing*, 4(6):pp799–813, June 1995.

[3] Wolfgang J. T. Spyra, Adel Faridani, Kennan T. Smith, and Erik L. Ritman. "Computed tomographic imaging of the coronary arterial tree - Use of local tomography". *IEEE Transactions on Medical Imaging*, 9(1):pp1–4, March 1990.

[4] Berkman Sahiner and Andrew E. Yagle. "Region-of-Interest Tomography using Exponential Radial Sampling". *IEEE Transactions on Image Processing*, 4(8):pp1120–1127, August 1995.

[5] Stanley R. Deans. *The Radon Transform and Some of Its Applications*. John Wiley and Sons, USA, 1983.

[6] G. Deslauriers and S. Dubuc. "Symmetric iterative interpolation processes". *Constructive approximation*, 5:49–68, 1989.

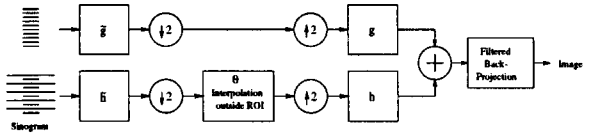

(a) The reconstruction algorithm of Wavelet localized tomography.

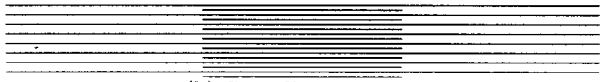

(b) Sampling pattern.

Figure 1. One level Wavelet localized tomography.

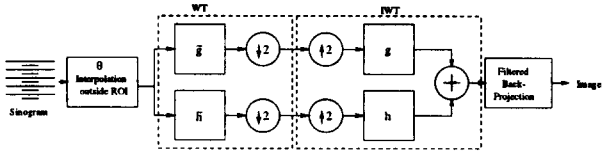

Figure 2. Modified ROI reconstruction.

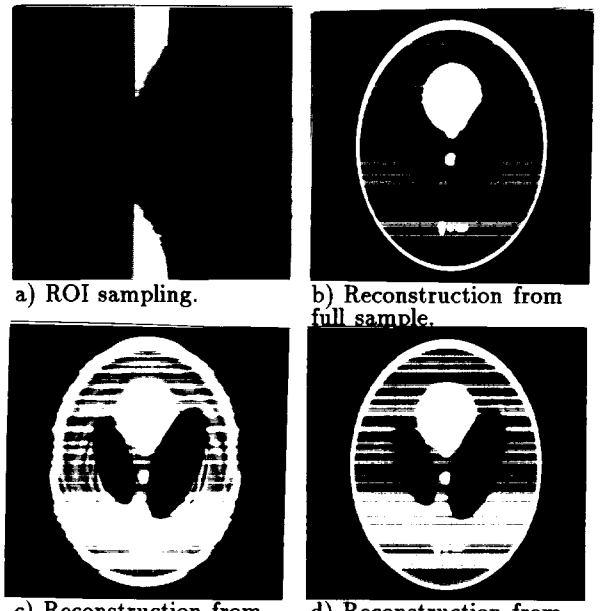

a) ROI sampling.

b) Reconstruction from full sample.

c) Reconstruction from Wavelet Localization.

d) Reconstruction from Linear Interpolation.

Figure 3. Results of using different approaches to reconstruct the ROI.

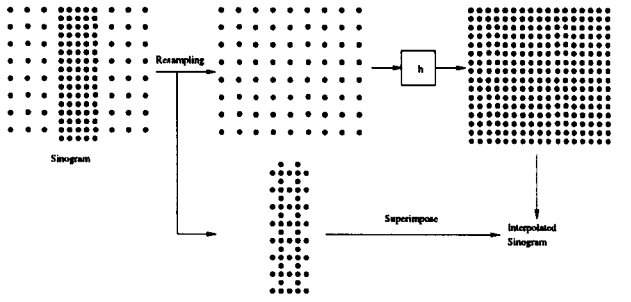

Figure 4. An outline of the proposed multiresolution interpolation algorithm.

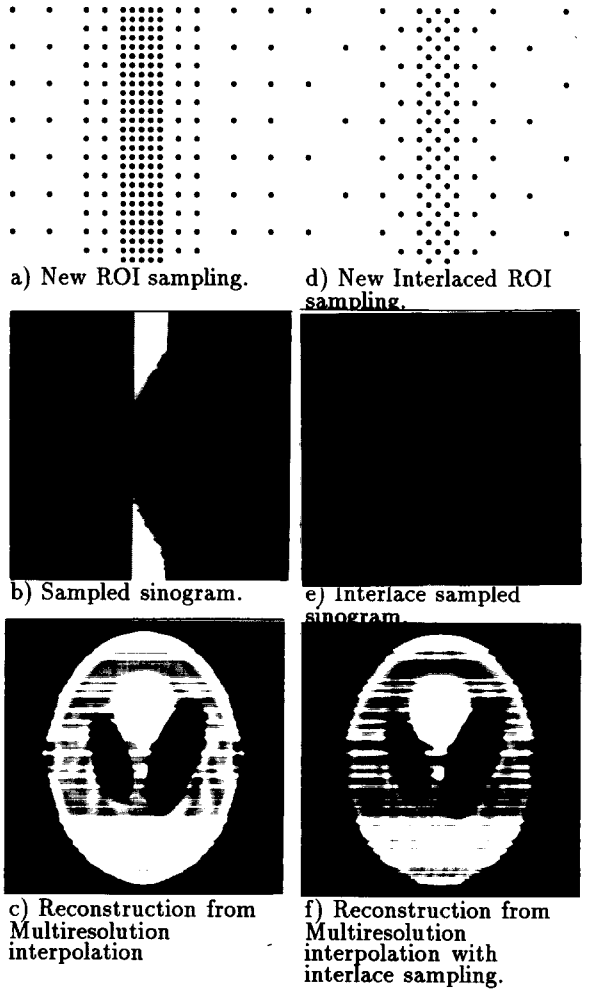

a) New ROI sampling.

d) New Interlaced ROI sampling.

b) Sampled sinogram.

e) Interlace sampled sinogram.

c) Reconstruction from Multiresolution interpolation

f) Reconstruction from Multiresolution interpolation with interlace sampling.

Figure 5. Results of using the new sampling scheme.